Preprints of the 18th IFAC World Congress
Milano (Italy) August 28 - September 2, 2011

Trajectory Tracking of Vision Based Robot Systems Using Piecewise Continuous Controllers and Observers

Haoping Wang†*, Christian Vasseur*, Vladan Koncar, and Nicolai Christov*,**

†Université de Picardie Jules Verne, MIS, 7 Rue du Moulin Neuf, Amiens, France
**Université Lille 1 : Sciences et Technologies, LAGIS, Bât. P2, 59655 Villeneuve d'Ascq, France*
(e-mail: haoping.wang ; christian.vasseur; nicolas. christov@univ-lille1.fr).
***ENSAIT, GEMTEX, 9 rue de l'Ermitage, BP 30329, 59056 Roubaix, France*
(e-mail: vladan.koncar@ensait.fr)

Abstract: This paper deals with a new approach of trajectory tracking for a X-Y robot by using the sampled and delayed output of a low cost vision system. The proposed approach is based on the theory of piecewise continuous systems which constitute a particular class of hybrid systems with autonomous switching and controlled impulses. A new robust trajectory tracking system, consisting of a specific piecewise continuous controller and a piecewise continuous observer, is developed. Real-time results are given to illustrate the effectiveness and robustness of the new robot control system.

Keywords: Piecewise continuous systems, Piecewise continuous controllers, Piecewise continuous observer, vision based X-Y robots

1. INTRODUCTION

Nowadays, Computer Numerical Controlled (CNC) tools are widely used in manufacturing automation. For instance, workpieces in the machining centers are placed on an X-Y table and two-axis motion CNC systems are part of the mainstream configuration (Park et al. 2003). During the last few years, one of the recent advances in this field is the use of direct drive X-Y table systems (Liu et al. 2005). In comparison with the conventional gear reduction systems, direct drive systems offer lower friction and higher mechanical stiffness, and thus are very suitable for high speed and high acceleration applications. Recently, many kinds of robust motion control schemes for X-Y table based robot accurate positioning have been proposed: a fuzzy control (Kung et al. 2009), a neural network based control (Lin et al. 2004), a numerical adaptive fuzzy control (Tsai et al. 2006), a composite nonlinear feedback control consisting of linear and nonlinear feedbacks without switching element (Cheng et al. 2007), an integral sliding mode control (Chen et al. 2007), etc.

A considerable amount of research has also been done in the field of vision based mechanical systems control (Hutchinson et al. 1996, Monroy et al. 2007, Xu et al. 2009, Tsai et al. 2009, Tamadazte et al. 2009, Hu et al. 2010). The interest for this class of systems is motivated by the need of supervision and remote control, and by the fact that they ensure more flexible contactless wiring and improved signal/noise ratio (Monroy et al. 2007). As it is well known, the introduction of visual sensors often deliver sampled and delayed signals due to their digital nature and computation-transfer time (e.g. image processing) respectively. In vision based X-Y robots,

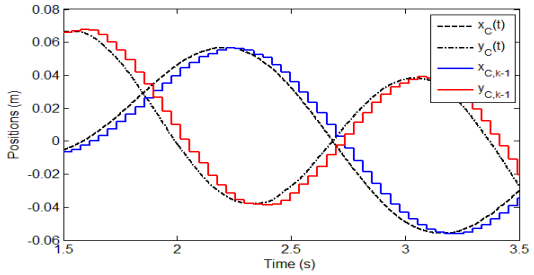

Fig. 1. Measurement signals: (x_C, y_C) and $(x_{C,k-1}, y_{C,k-1})$

the vision system determines the robot position coordinates (x_C, y_C) and transmits them to the control computer. The available information for the control system is thus the sampled and delayed signal $(x_C(kt_e - T_e), y_C(kt_e - T_e)) = (x_{C,k-q}, y_{C,k-q})$ where t_e is the camera sampling period, $T_e = qt_e$ represents the delay corresponding to the time necessary for image data acquisition, processing and transfer and *k, q* are integers. For the considered in this paper low cost vision system one has $t_e = 40$ ms and $q = 1$, and the robot position measurements are denoted by $(x_{C,k-1}, y_{C,k-1})$. An example form of (x_C, y_C) and $(x_{C,k-1}, y_{C,k-1})$ is given in Fig. 1. The challenge here is to realize a robust trajectory control of the vision based X-Y robot using the sampled and delayed signal $(x_{C,k-1}, y_{C,k-1})$. To solve this problem we propose in this paper a robot control system based on the theory of the Piecewise Continuous (PC) systems and consisting of a PC controller (PCC) and a PC observer (PCO).

Copyright by the
International Federation of Automatic Control (IFAC)

The paper is organized as follows. First, the PC systems are introduced in Section II. Then, in Section III a new PCC is developed by enabling switching at high frequencies. In order to estimate the robot position, a PCO is proposed in Section IV. The experimental vision based X-Y robot platform is described in Section V and real time trajectory tracking results are presented in Section VI. Finally, in Section VII some concluding remarks are given.

2. PIECEWISE CONTINUOUS SYSTEMS

The PC systems (PCS) which were first introduced in (Koncar et al. 2003) are characterized by two input spaces and two time spaces. The first time space is the discrete time space $S=\{t_i, i=0,1,2,\cdots\}$ called switching space. The second one is the continuous time space $\Phi_t=\{\Im-S\}$ where $\Im=\{t\in[0,\infty]\}$. Each input corresponds to one specific time space. At each switching instant, the plant is controlled from the first input space V^σ. Between two switching instants, the plant is controlled from the second input space U^r. Two successive switching instants t_i and t_{i+1} delimit a piece noted $\Phi_i=\{\Phi_t \mid \forall t\in]t_i,t_{i+1}[\}$. Thus for $t_i=iT_e$, the state-space based approach makes possible to describe a Linear PCS (LPCS) as

$$x(iT_e^+)=B_d v(iT_e),\ \forall t\in S \tag{1a}$$
$$\dot{x}(t)=Ax(t)+B_c u(t),\ \forall t\in\Phi_t \tag{1b}$$
$$y(t)=Cx(t),\ \forall t\in\Im \tag{1c}$$

where $S=\{iT_e, i=0,1,2,\cdots\}$, $x(t)\in\Re^n$ is the system state vector, $y(t)\in\Re^m$ is the output vector, $v(t)\in\Re^\sigma$ and $u(t)\in\Re^r$ are the input vectors, $A\in\Re^{n\times n}$ is the system state matrix, $B_c\in\Re^{n\times r}$ and $B_d\in\Re^{n\times\sigma}$ are the input matrices, and $C\in\Re^{m\times n}$ is the output matrix. At switching instants the system state changes according to the linear algebraic relation (1a) and the continuous-time state evolution is described by the linear differential equation (1b). Fig. 2 illustrates the LPCS structure and symbolic representation.

Integrating (1b) in $\Phi_i=\{\Phi_t \mid \forall t\in]iT_e,(i+1)T_e[\}$ and taking into account (1a), one obtains

$$x(t)=\exp\big(A(t-iT_e)\big)B_d v(iT_e)+\int_{iT_e}^{t}\exp A(t-\tau)B_c u(\tau)d\tau,\ \forall t\in\Phi_i. \tag{2}$$

The left limit $x(iT_e^-)$ of $x(t)$ at $t=iT_e$ is deduced from (2) for the interval Φ_{i-1}:

$$x(iT_e^-)=\exp\big(A(t-iT_e)\big)B_d v\big((i-1)T_e\big)+\int_{(i-1)T_e}^{iT_e}\exp A(t-\tau)B_c u(\tau)d\tau. \tag{3}$$

Thus in the general case $x(iT_e^-)\neq x(iT_e^+)$. An example state evolution of a 1st order system with T_e=1s and B_d=1 is shown in Fig. 3. According to the classification of (Tittus et al. 1998), this class of control systems has hybrid properties. Moreover, according to Branicky taxonomy (Branicky et al. 1998), PCS are hybrid systems with autonomous switching and controlled impulses. Based on the PCS theory, a PC

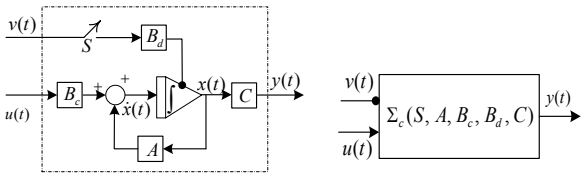

(a) System structure (b) Symbolic representation

Fig. 2. Linear piecewise continuous systems

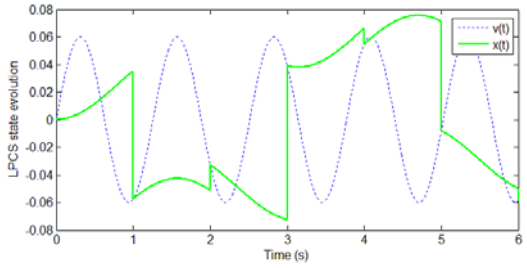

Fig. 3. LPCS state evolution for switching period T_e=1s

controller requiring a linear plant model was developed in (Koncar et al. 2003). In this paper we propose a new class of PC controllers which allow controlling the plant without knowledge of its model. The new controller can be easily implemented and makes possible to realize robust output trajectory tracking of the vision based X-Y robot.

The analysis of the existing vision based control systems shows that the delaying and sampling of the camera signal are not sufficiently compensated. That is why in Section IV we develop a PC observer which gives a continuous undelayed estimate of the x-y robot position.

Further on, the discrete values of every function $f(t)$ will be considered as being sampled with T_e period and to simplify the notations $f(iT_e)$ will be denoted as f_i. Moreover, if some signal $f(t)$ is discontinuous, we shall consider the right value at the discontinuity since the switching at each iT_e imply consequences at iT_e^+. For simplification, the notation $f_i^+=f(iT_e^+)$ will be used.

3. PIECEWISE CONTINUOUS CONTROLLER

In this section, we first present the existing PCC and the sampled trajectory tracking strategy used to determine the controller parameters. Then we derive a new PC controller by enabling switching at high frequencies, i.e. for $T_e\to 0^+$.

PCC was introduced in (Koncar et al. 2003) and is described as

$$\lambda_i^+=\delta\psi_i,\ \forall t\in S \tag{4a}$$
$$\dot{\lambda}(t)=\alpha\lambda(t)+\beta\varphi(t),\ t\in\Phi_t \tag{4b}$$
$$u(t)=\gamma\lambda(t),\ t\in\Im \tag{4c}$$

where $\lambda(t)\in\Re^n$, $\psi(t)\in\Re^s$ and $\varphi(t)\in\Re^r$ the PCC state and inputs, respectively. Equation (4a) defines the controller state $\lambda(t)$ at switching instants by means of the discrete time input

$\psi(t)$ and the linear transformation matrix $\delta \in \Re^{n\times s}$. Equation (4b) describes the continuous-time evolution of the controller state under the action of the continuous time input $\varphi(t)$. Here $\alpha \in \Re^{n\times n}$ and $\beta \in \Re^{n\times r}$ are the state matrix and the input matrix of the controller. For a simplified PCC, β can be imposed zero and in this case the only parameter defining the controller state behavior in Φ_i is α which is chosen so as to ensure the stability of the controller. Equation (4c) is the output equation of the controller, where $\gamma \in \Re^{r\times n}$ is the output matrix. The output $u(t) \in \Re$ is the control signal to be applied to the plant. According to the LPCS description in Section 2, in general $\lambda_i^+ \neq \lambda_i^-$.

Consider the application of PCC to a plant modeled as

$$\dot{x}(t) = Ax(t) + Bu(t) \tag{5a}$$

$$y(t) = Cx(t) \tag{5b}$$

$$\theta_{k-1} = y_{k-1} \tag{5c}$$

where $x(t) \in \Re^n$, $u(t) \in \Re$, $y(t) \in \Re$ are respectively the plant state, input and output, respectively, and θ_{k-1} are the delayed and sampled output measurements to be used by the controller. Without loss of generality we assume that $C = [1\,0\ldots 0]$. The closed loop system (5), (4) is then described as

$$\dot{x}(t) = Ax(t) + Bu(t),\ t \in \Im \tag{6}$$

$$\lambda_i^+ = \delta\psi_i, i \in S \tag{7}$$

$$\dot{\lambda}(t) = \alpha\lambda(t),\ t \in \Im - S \tag{8}$$

$$u(t) = \gamma\lambda(t),\ t \in \Im. \tag{9}$$

The tuning of PCC consists of determining $\psi(t)$ and δ so as to achieve sampled tracking of a desired trajectory $c_s(t)$ by the plant state $x(t)$ with one sampling period of delay:

$$x_{i+1} = c_{s,i},\ i = 0,1,2,... \tag{10}$$

Equations (6)-(8) allow us to express the state value x_{i+1} as a function of x_i:

$$x_{i+1} = A_d x_i + M\lambda_i^+ \tag{11}$$

where $A_d = e^{AT_e}$ and $M = A_d\int_0^{T_e} e^{-A\tau}B\gamma e^{\alpha\tau}d\tau$.

From (11) and (6) we obtain the relation

$$\lambda_i^+ = M^{-1}\left\{c_{s,i} - A_d x_i\right\} \tag{12}$$

which gives the switching value of the controller state under the condition that M^{-1} exists. Therefore the sampled tracking of $c_s(t)$ can be ensured for

$$\delta = M^{-1} \text{ and } \psi(t) = c_s(t) - A_d x(t). \tag{13}$$

The performance of PCC (4), (13) can be enhanced by enabling switching at high frequencies, i.e. for $T_e \to 0^+$. Consider the case of sampled output tracking

$$y_{i+1} = c_{o,i},\ i = 0,1,2,... \tag{14}$$

where $c_o(t)$ is the desired output trajectory. In this case a first order PCC is used and then from (11) one obtains

$$y_{i+1} = CA_d x_i + CA_d\int_0^{T_e} e^{-A\tau}B\gamma e^{\alpha\tau}d\tau\lambda_i^+ \tag{15}$$

where $\lambda_i \in \Re$, $\alpha \in \Re$ and $\gamma \in \Re$. For $T_e \to 0^+$ and using first order approximation one has

$$y_{i+1} = \Upsilon x_i + \Upsilon\int_0^{T_e}(I_n - A\tau)B\gamma(1+\alpha\tau)d\tau\lambda_i^+ \tag{16}$$

where $\Upsilon = C(I_n + AT_e)$ and I_n is the n^{th} order unit matrix. We can thus rewrite (16) as

$$y_{i+1} = y_i + CAT_e x_i + \left(CB\gamma T_e + \varepsilon(T_e^2)\right)\lambda_i^+ \tag{17}$$

where $\varepsilon(T_e^2)$ is negligible when $T_e \to 0^+$ .From (17) and (14) we have

$$\left(CB\gamma T_e + \varepsilon(T_e^2)\right)\lambda_i^+ = c_{o,i} - y_i - CAT_e x_i \tag{18}$$

which enable us to evaluate the initial condition of the PCC state at each switching instant. In order to solve (18) numerically, we rewrite it as

$$\lambda_i^+ - \left(\lambda_i^+ - \left(CB\gamma T_e + \varepsilon(T_e^2)\right)\lambda_i^+\right) = c_{o,i} - y_i - CAT_e x_i. \tag{19}$$

With fast switching ($T_e \to 0^+$), equation (19) becomes

$$\lambda_i^+ = I^-\lambda_i^+ + c_{o,i} - y_i \tag{20}$$

where $I^- = 1 - \left(CB\gamma T_e + \varepsilon(T_e^2)\right)$. Equation (20) can be interpreted algorithmically as an iterative evaluation of λ_i^+ at each calculation step:

$$\lambda_i^+ \leftarrow I^-\lambda_i^+ + c_{o,i} - y_i. \tag{21}$$

Thus for fast switching the calculation of the PCC initial condition at each switching instant is highly simplified: for $T_e \to 0^+$ the evolution of the controller state is negligible and PCC can be regarded as a Zero Order Hold (ZOH). If switching occurs at each calculation step of the computer, the ZOH can be replaced by a simple circuit as shown in Fig. 4. Thus the new PC controller doesn't require a plant model which is a major advantage in comparison with the existing

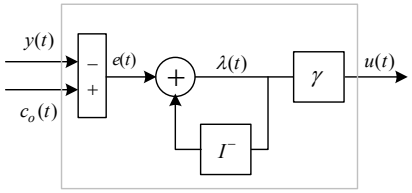

Fig. 4. New piecewise continuous controller

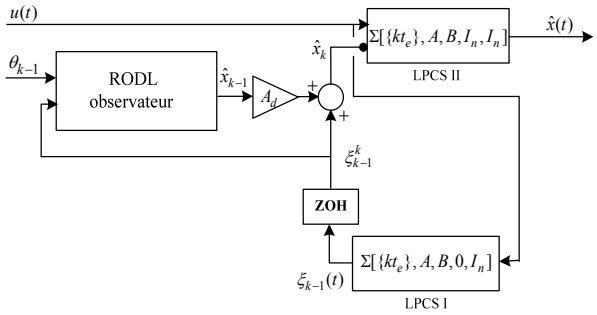

Fig. 5. Piecewise continuous observer

PCC. However, a continuous feedback is required.

4. PIECEWISE CONTINUOUS OBSERVER

In this section we derive a PC observer which makes possible to estimate the plant continuous state $x(t)$ using the sampled and delayed measurements θ_{k-1}. The proposed PCO consists of two LPCS and a Reduced Order Discrete time Luenberger (RODL) observer (Luenberger et al. 1971) connected as shown in Fig. 5 where the matrices *A*, *B* and *C* in LPCS I and LPCS II are defined in (5).

According to (3) for LPCS I one has

$$x(t) = \int_{(k-1)t_e}^{t} \exp A(t-\tau)Bu(\tau)d\tau \;=\; \xi_{k-1}(t),\;\; t \in \Phi_{k-1}. \tag{22}$$

Thus at each $t = kt_e$ one obtains the signal

$$\xi^k_{k-1} = \int_{(k-1)t_e}^{kt_e} \exp A(kt_e-\tau)Bu(\tau)d\tau = \begin{bmatrix} \xi^k_{1,k-1} \\ \xi^k_{2,k-1} \end{bmatrix} \tag{23}$$

where $\xi 1^k_{k-1} \in \Re$ and $\xi 2^k_{k-1} \in \Re^{(n-1)}$.

Denoting $x_k = [\theta_k \; w_k^T]^T$ and $A_d = \begin{bmatrix} A_{11} & A_{12} \\ A_{21} & A_{22} \end{bmatrix}$, $A_{11} \in \Re$, the vector $w_{k-1} \in \Re^{n-1}$ is estimated by using the RODL observer

$$z_k = Fz_{k-1} + G\theta_{k-1} + (\xi^k_{2,k-1} - L\xi^k_{1,k-1}) \tag{24a}$$

$$z_{k-1} = \hat{w}_{k-1} - L\theta_{k-1} \tag{24b}$$

where

$F = A_{22} - LA_{12}$,

$G = (A_{22} - LA_{12})L + (A_{21} - LA_{11})$,

and $L \in \Re^{n-1}$ is determined to ensure the observer stability, thus the convergence of $\hat{w}_k$ to w_k. Estimating w_{k-1} as $\hat{w}_{k-1} = z_{k-1} + L\theta_{k-1}$, one gets $\hat{x}_{k-1} = [\theta_{k-1} \; \hat{w}^T_{k-1}]^T$. Then $\hat{x}_k$ is estimated integrating (6) in the Φ_{k-1} piece:

$$\hat{x}_k = A_d\hat{x}_{k-1} + \xi^k_{k-1}. \tag{25}$$

The continuous time state estimate $\hat{x}(t)$ is the output of LPCS II:

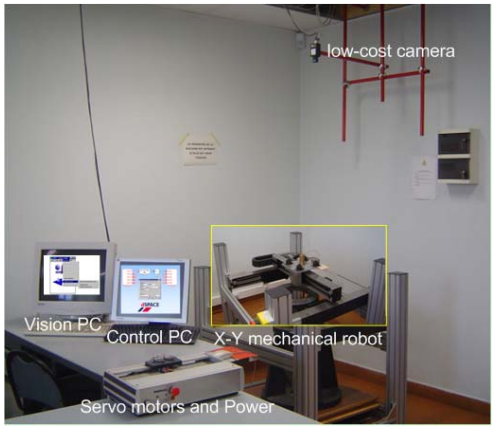

Fig. 6. Vision based X-Y robot platform

$$\hat{x}(t) = A_d\hat{x}_k + \int_{kt_e}^{t} \exp A(t-\tau)Bu(\tau)d\tau\,. \tag{26}$$

5. VISION BASED X-Y ROBOT PLATFORM

The proposed PC control system has been implemented and tested on the vision based X-Y robot platform shown in Fig. 6 and contains the following parts:

1) A mechanical system composed of an X-Y aluminum chassis, enabling only 48 cm displacement on each axis. The x-axis moves along the y-axis. Axes are actuated by AC motors via notched belt.

2) A vision system of a low cost IR CCD (Jai M50 IR) camera with a sampling rate of 25 frames/sec and a low resolution of 640 × 480 pixels configured in non-interlaced mode. This camera is linked to a vision computer which is equipped with an image acquisition card (ELTEC PC-EYE 4) and image processing software (TEKVIS).

3) A controller designed through Matlab/Simulink and implemented on the dSpace card DS1103 via ControlDesk. The control signals are sent to a power amplifier via ± 10 V DAC.

4) Two servo motors (SANYO DENKI PY2A015A3-A3) and two AC motors (P50B050020-DXS00M) driven by a dSpace computer input/output card via a power amplifier supplied with 240 V. The AC motors deliver a nominal couple of 3.0 Nm with a power of 200 W. The platform returns the cart's continuous positions (x_C, y_C) by means of a 8 μm resolution incremental encoders equipped with the AC motors.

On the x-axis, the motor-cart is modeled as

$$\ddot{x}_C = (-\dot{x}_C + k_x u_x)/\tau_x \tag{27}$$

where u_x is the motor input voltage, x_C is the robot displacement, k_x is the overall gain of the motor-cart on x-axis and τ_x is the time constant of the motor-cart on x-axis. In the same way, we can model the motor-cart on y-axis. For the platform considered, $\tau_x = \tau_y = 0.008$s and $k_x = k_y = 2.92$.

The vision system determines the X-Y robot position coordinates (x_C, y_C) and transmits them to the control

computer via the RS-232 serial communication port. The measurements of the camera are available at a sampling rate of $T = 40$ ms (acquisition-processing-transfer time). An infrared LED has been placed on the robot as illustrated in Fig. 6 so as to facilitate its localization in the X-Y plan by the IR camera. In order to synchronize the camera with the controller, the camera is triggered by an external periodical pulse signal generated via the dSpace card. Moreover, in view of enhancing the camera as a sensor, the latter is calibrated by a four step TSAI calibration procedure (Heikkila et al. 1997) which is included in the control. This calibration also compensates the deformations caused by the camera lens. Under these conditions the visual measurements $(x_{C,k-1}, y_{C,k-1})$ of the robot position coordinates (x_C, y_C) are obtained.

As the X-Y robot structure is symmetrical, for simplification sake, only the x-axis control is considered. According to (27) the state space robot model can be written as

$$\dot{x}(t) = Ax(t) + Bu(t)$$
$$y(t) = Cx(t)$$
$$\theta_{k-1} = x_{C,k-1}$$

where $x(t) = \left[x_C(t) \quad \dot{x}_C(t)\right]^T$, $u(t) = u_x(t)$, $y(t)$ are the robot state, input and output, respectively, θ_{k-1} are the delayed and sampled measurements of the cart displacement, and

$$A = \begin{bmatrix} 0 & 1 \\ 0 & -1/\tau_x \end{bmatrix}, \quad B = \begin{bmatrix} 0 \\ k_x/\tau_x \end{bmatrix}, \quad C = \begin{bmatrix} 1 & 0 \end{bmatrix}.$$

6. EXPERIMENTAL RESULTS

The structure of the proposed vision based trajectory tracking control system is shown in Fig. 7. For PCO, $F_x = F_y = 0$, $G_x = G_y = -0.848$ and $L_x = L_y = 0.848$ were determined and for

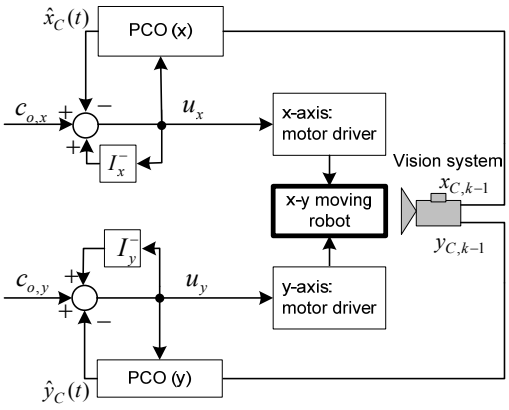

Fig. 7. Tracking control system of vision based x-y robot

PCC $I_x^- = I_y^- = 0.92$ and $\gamma_x = \gamma_y = 1$ were chosen. The desired output trajectories for each axis are defined as

$$\begin{bmatrix} c_{o,x} \\ c_{o,y} \end{bmatrix} = \begin{bmatrix} \cos\alpha & -\sin\alpha \\ \sin\alpha & \cos\alpha \end{bmatrix} \begin{bmatrix} m\sin\omega_x t \\ n\sin(\omega_y t + \varphi) \end{bmatrix} \tag{28}$$

where α (rad) is the oblique angle, m and n (m) are amplitudes, ω_x and ω_y (rad/s) are the imposed frequencies for each axis and φ (rad) is the phase. During the experiments, the parameters were first chosen as $(\alpha, m, n, \omega_x, \omega_y, \varphi) = (0.33\pi, 0.04, 0.06, 5, 10, 0.5\pi)$ defining a circle.

The corresponding real-time results are given in Fig. 8 and 9 where $x_C(t)$ and $y_C(t)$ are the continuous X-Y robot position coordinates measured by encoders, $\hat{x}_C(t)$ and $\hat{y}_C(t)$ are the X-Y robot coordinates estimated by PCO, and $x_{C,k-1}$ and $y_{C,k-1}$ are the sampled and delayed measurements obtained by the camera. Fig. 8 shows that the proposed PCO compensates very well sampling and delaying effects of the low cost vision system on x-axis. Moreover, from Fig. 9a (which shows $c_{o,x}$, $c_{o,y}$ and $x_C(t)$, $y_C(t)$) one can conclude that the proposed tracking controller ensures a perfect tracking of the desired output reference. In order to test the robustness of the proposed control system, a perturbation was introduced by hiding the IR LED for an instant (thus breaking the feedback loop). The corresponding results are given in Fig. 9b.

Then the parameters in (28) were chosen as $(\alpha, m, n, \omega_x, \omega_y, \varphi) = (0.67\pi, 0.04, 0.04, 2.5, 7.5, 0.5\pi)$ defining a Lissajous curve. The results of tracking this reference, with and without perturbation, are illustrated in Fig. 10. The tests results demonstrate the efficiency and the robustness of the proposed control system when the camera drops out some measurements. Illustrative videos are available at http://www-lagis.univ-lille1.fr/~wang/Research_eng.html

6. CONCLUSIONS

A new approach for trajectory tracking control of vision based X-Y robots is proposed based on the theory of piecewise continuous systems. The developed control system uses sampled and delayed data from a low cost CCD camera and consists of specific piecewise continuous controller and piecewise continuous observer. This control system can be easily implemented and ensures robust output trajectory tracking.

REFERENCES

The authors gratefully acknowledge financial support by European Union through the INTERREG IVA -- SCODECE (Smart Control and Diagnosis for Economic and Clean Engine) project and ARCUS international research project.

REFERENCES

Branicky, M. S., Borkar, V. S., and Mitter, S. K. (1998). A unified framework for hybrid control: model and optimal control theory. *IEEE Trans. Autom. Contr.*, 43(1), 31-45.

Cheng, G., Peng, K., Chen, B. M., and Lee, T. H. (2007). Improving transient performance in tracking general references using composite nonlinear feedback control and its application to high-speed XY-table positioning

mechanism. *IEEE Trans. Ind. Electron.*, 54(2), 1039-1051.

Chen, S.L., and Wu, K.C. (2007). Contouring control of smooth paths for multiaxis motion systems based on equivalent errors. *IEEE Trans. Contr. Syst. Technol.,* 15(6), 1151-1158.

Heikkila, J., and Silven, O. (1997). A four-step camera calibration procedure with implicit image correction. *Proc. Conf. on Computer Vision and Pattern Recognition,* pp.1106-1112

Hu, G.Q., Gans, N., Fitz-Coy, N., and Dixon, W. (2010). Adaptive homography-based visual servo tracking control via a quaternion formulation. *IEEE Trans. Control Syst. Technol.*, 18(1), 128-135.

Hutchinson, S., Hager, G.D., and Corke, P.I. (1996) A tutorial on visual servo control. *IEEE Trans. on Robot. Autom.* 12(5), 651-670.

Koncar, V., and Vasseur, C. (2003). Control of linear systems using piecewise continuous systems. *IEE Control Theory & Appl.* 150(6), 565-576.

Kung, Y.S., Fung, R.F., and Tai, T.Y. (2009). Realization of a motion control IC for X-Y Table based on novel FPGA Technology. *IEEE Trans. Ind. Electron.* 56 (1), 43-53.

Lin, F.J., Wai, R.J., and Huang, P.K. (2004). Two-axis motion control system using wavelet neural network for ultrasonic motor drives. *IEE Proc.-Electr. Power Appl.* 151 (5), 613-621.

Liu, Z.Z., Luo, F.L., and Rahman, M.A. (2005). Robust and precision motion control system of linear-motor direct drive for high-speed X-Y Table positioning mechanism. *IEEE Trans. Ind. Electron.* 52 (5), 1357-1363.

Luenberger, D.G. (1971). An introduction to observers. *IEEE Trans. Automat. Contr.* 16(6), 596-602.

Monroy, G., Kelly, R., Arteage, M., and Bugarin, E. (2007). Remote visual servoing of a robot manipulator via Internet2. *Journal of Intelligent and Robotic Systems*. 49 (2), 171-187.

Park, E.C., Lim, H., and Choi, C. H. (2003). Position control of X-Y table at velocity reversal using Presliding friction characteristics. *IEEE Trans. Control Syst. Technol.* 11 (1), 24-31.

Tamadazte, B., Arnould, T., Dembélé, S., Le Fort-Piat, N., and Marchand, E. (2009). *Real-time vision-based microassembly of MEMS.* IEEE/ASME Inter. Conf. Advanced Intel. Mechatronics, Singapore.

Tittus, M., and Egart, B. (1998). Control Design for Integrator Hybrid Systems. *IEEE Trans. Automat. Contr.* 43 (4), 491-500.

Tsai, C.Y., and Song, K.T. (2009). Visual tracking control of a wheeled mobile robot with system model and velocity quantization robustness. *IEEE Trans. Control Syst. Technol.* 17 (3), 520-527.

Tsai, M.H., Kung, Y.S., and Huang, C.C. (2006). Development of a servo system for linear X-Y table based on DSP controller. *Proc. 2006 IEEE Int. Conf. Ind. Technol.*, pp. 2907-2912.

Xu, Y.J., and Ritz, E. (2009). Vision based flexible beam tip point control. *IEEE Trans. Control Syst. Technol.* 17(5), 1220-1227.

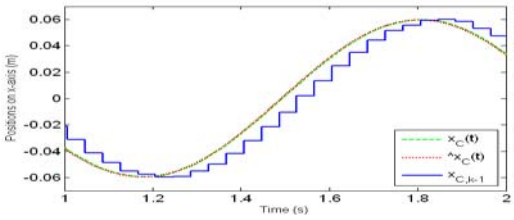

Fig. 8. Piecewise Continuous Observer on x-axis

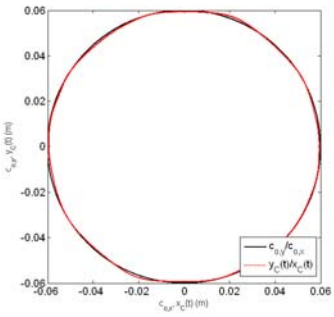

(a) without perturbation

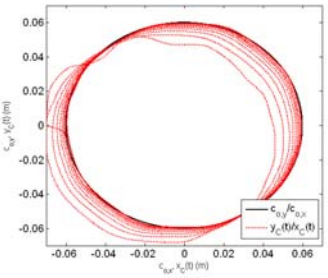

b) with perturbation

Fig. 9. Tracking a circle trajectory under different conditions

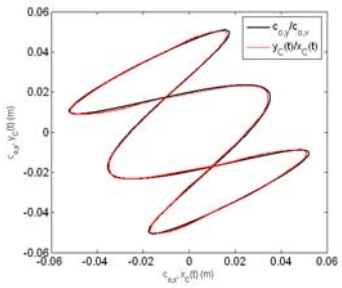

(a) without perturbation

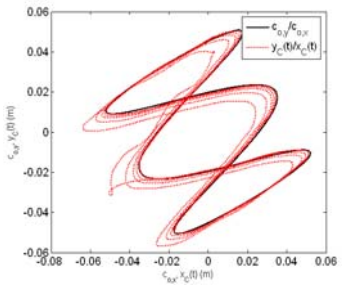

(b) with perturbation

Fig. 10. Tracking a Lissajous curve under different conditions